Electronic structure of thin heterocrystalline superlattices in SiC and AlN

M. S. Miao and Walter R. L. Lambrecht
Department of Physics, Case Western Reserve University, Cleveland, Ohio 44106-7079, USA
(Received 18 June 2003; published 21 October 2003)

The spontaneous polarization, the valence band offset, and the quantum confinement effect for thin SiC and AlN cubic/hexagonal heterocrystalline superlattices are studied by use of a full potential linear muffin-tin orbital method (FP-LMTO). We find that the polarization is screened and suppressed while the length of the cubic region grows. The band offsets do not change with layer thickness. For thin superlattices, the quantum confinement effects dominate and result in a band gap which stays larger than the gap of the bulk cubic structure. Furthermore, the energy levels of the bound states in the quantum well resemble the pattern of the energy levels of conventional III-V based quantum wells and superlattices but at a much smaller length scale, which is due to the higher quantum well depth and the larger effective masses in SiC and AlN systems.

DOI: 10.1103/PhysRevB.68.155320 PACS number(s): 73.21.Cd, 71.20.Nr

One of the pronounced features of SiC is the systematic variation of the band gap with polytype. This feature led Bechstedt *et al.*[1] to propose heterocrystalline superlattices (HCSL). Surprisingly, they found that these heterocrystalline structures had band gaps smaller than bulk 3C. It was explained as a consequence of their type-II band-offset character and the appearance of a linear contribution to the electrostatic potential caused by the charge localized at the interface[2] between materials with and without spontaneous polarization. Recently, 4H/3C and 6H/3C quantum wells have been grown successfully by molecular beam epitaxy (MBE).[3,4] The photoluminescence measurements exhibit features consistent with a gap smaller than that of bulk 3C. A rough estimation based on a triangular quantum well due the spontaneous polarization appears to explain these observations.[4] However, PL features below the band gap may also be related to defect bound excitons. Similar studies have also been performed for AlN and SiC HCSL using LMTO within the atomic sphere approximation (ASA).[2] ASA results support that the superlattice band gap could be smaller than 3C but according to our own experience may overestimate the spontaneous polarization effect.

Another motivation for studying the heterocrystalline structures stems from the recent observations of stacking fault (SF) growth in 4H SiC diodes under forward bias[5,6] and in annealed heavily *n*-type doped epilayers.[7–9] The growth of the double stacking faults (DSF's) can result a six-layers cubic inclusion in 4H SiC. The localized electron states near the conduction band minimum can trap electrons and can cause a driving force toward increasing the SF area in *n*-type SiC.[10] The electronic structures of double and triple SF have been calculated and the gaps obtained are all larger than those in pure 3C.[11–13]

As shown in Fig. 1, the gap of the 3C/2H HCSL is determined by (1) the quantum confinement effect of the electron states caused by the conduction band offset (CBO), (2) the occurrence of a linear contribution to the potential caused by the accumulation of the charges at the interfaces between materials with different spontaneous polarization, and (3) the type band offsets of the valence bands. If the VBO is of type II, and the spontaneous polarization effect latter is prominent, the band gap of the superlattice could become smaller than that of the bulk phase with the smaller band gap. Otherwise, if the confinement effect dominates, the gap will be larger than that of 3C. On the other hand, it is interesting to see how the properties of the SL changes with the layer thickness. In this paper, we define the SL size based on the layer type and perform a series of calculations with growing number of cubic inclusion layers. The changes of the quantum confinement, the polarization effect, and the VBO versus the layer thickness will be carefully analyzed. This is crucial to resolve the conflicting results on the band gaps. We choose here the simplest case of the 3C/2H SL because it maximizes both the spontaneous polarization and the VBO effects. If no gaps smaller than 3C occur in this case, they can safely be ruled out also in the 3C/4H and 3C/6H cases.

In Refs. 1 and 2, the heterocrystalline structures are formed by attaching a few 3C units consisting each of three cubic layers with a 4H, 6H, or 2H region in such a way that the resulting cell is always hexagonal and such that the total size of the system is fixed. Inclusions of six, seven, or eight cubic layers are obtained in this manner depending on whether the hexagonal region is 2H, 4H, or 6H. In the stacking fault studies, the inclusion of cubic layers is defined by glide induced SF's.[10–13] The systems with one, two, or three SF's contain two, five, or six continuous cubic layers. In this paper, we define the HCSL by the number of continuous cubic and hexagonal layers. We calculated a series of HCSL's with an inclusion of one to twelve cubic layers in a

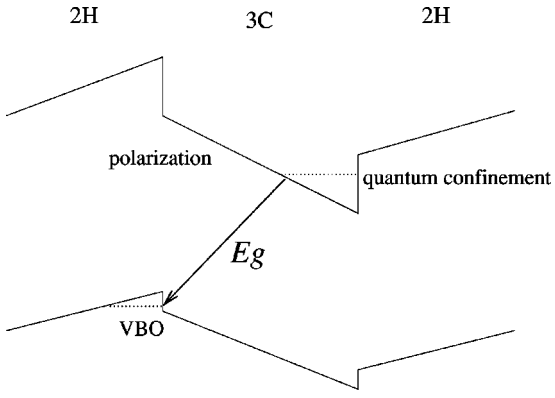

FIG. 1. The lineups of the VBM's and CBM's in the 3C and 2H regions of HCSL. The final band gap and the three major effects are denoted.

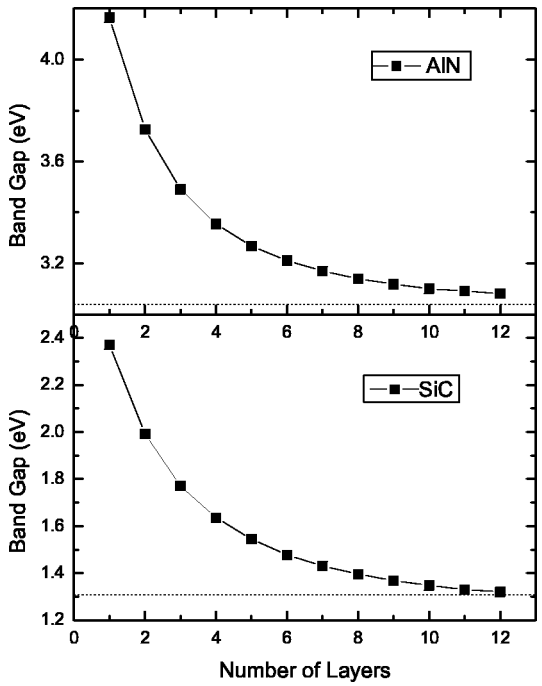

FIG. 2. The fundamental gap changes with the number of cubic layers in HCSL.

ten layer 2H region. In layer type notation (h or c) the one cubic layer HCSL is ($hhhhhchhhhh$). This can be converted to spin notation as ($\uparrow\downarrow\uparrow\downarrow\uparrow\downarrow\uparrow\downarrow\uparrow\downarrow$) or to ABC notation as $(ABABABACACA)C$. As a result, some of the systems are hexagonal and some of them are rhombohedral. Accordingly, we use $a_3=(0,0,mc/2),(-a/2,a\sqrt{3}/6,mc/2)$, or $(a/2,-a\sqrt{3}/6,mc/2)$ as the third lattice vector depending on the shape of the supercell, in which m is the total number of layers. This idea was first proposed in our previous study on stacking faults[10] to reduce the size of the model. It is more crucial here to use both rhombohedral and hexagonal cells because we want to sequentially increase the number of layers in the 3C region.

All the calculations are performed using a full-potential linear muffin-tin orbital method (FP-LMTO)[14]. The Hedin-Lundqvist local density functional[15] is employed as the exchange-correlation functional. A $4\times4\times4$ k mesh is used for the Brillouin zone integrations. Since atomic relaxations were found to be negligibly small, we performed all of the calculations reported here maintaining the c/a values and the parameter u for ideal SiC. This means that the tetrahedrons have no distortion in the z direction. This c/a value is slightly larger than that in real 4H and 6H structure but slightly smaller than that in real 2H. For AlN, the c/a and u values were fixed at the experimental values of 1.600 (Ref. 16) and 0.380, respectively, in the 2H part of the cell and kept ideal for the cubic layers. For evaluating the validity, we calculated the forces and found the largest force happens for the single cubic inclusion in 2H SiC QW and is only 7 mRy/au. This is below the usual convergence criterion for geometry relaxations.

Figure 2 shows the band gaps from the M point conduction band minimum to the Γ point valence band maximum. The conduction band minima for cubic SiC and AlN are at X point in the zinc blende Brillouin zone. While transformed to the wurtzite Brillouin zone, the original X point is located in between the M and L points. Because the cells used in this paper are all very long along the z direction, the bands have been folded many times along M-L line and become very flat. Thus, one can use directly the value at the M point without making a significant error. The 3C band gaps are also calculated in this way by using a 12 layer long hexagonal cell and are found to be 1.309 and 3.040 eV for SiC and AlN, respectively. These values underestimate the experimental value of 2.417 eV (Ref. 17) in SiC and the expected experimental gap in 3C-AlN (4.9 eV) (Ref. 18) by 1–2 eV as is usual because of the LDA.

The results depicted in Fig. 2 show that the band gaps for 3C inclusions in 2H superlattices decrease monotonically and asymptotically approach the gap value of bulk 3C. Notably the band gap is never lower than that of 3C. This is a result in contrast to Refs. 1,2 but agrees with Ref. 12 and our recent results[13] for 3C inclusions in 4H. Our results indicate that the quantum confinement effect is more important than the spontaneous polarization and the valence band offsets for thin HCSL's. We also point out that using ASA instead of FP calculations, we found an interface state at $E_c-1.1$ eV and a second one at $E_c-0.3$ eV for the six cubic layer inclusion in 4H. This indicates that the disagreement with Ke *et al.*[2] is due to the ASA inaccuracies. In particular, as we next show it indicates that ASA overestimates the spontaneous polarization. Indeed the shape approximations of the ASA do not allow us to describe the charge distribution at the interface with sufficient accuracy.

According to the spontaneous polarization point of view, the net interface charge at the interface between 3C and 2H is fixed by their difference in bulk spontaneous polarization (zero in 3C and some finite value in 2H). This interface charge then leads to a linear potential for a single interface and a zig-zag potential in a periodic superlattice. The slope of this zig-zag potential is completely determined by the supposedly fixed interface charge and thus, the total potential difference between the two ends of the 3C region should increase with increasing thickness of the 3C region. Since the valence band maximum is then localized at the opposite end of the conduction band minimum of the quantum well, a gap smaller than the 3C gap and possibly even a zero band gap or metallic state would result for thick enough 3C inclusions. On the other hand, this is definitely counterintuitive since for a really thick 3C inclusion, one expects bulk 3C properties to develop. This is the basic problem we address in this paper.

To investigate the polarization effect, we show in Fig. 3 the average potential at the muffin-tin sphere radii for the Si spheres as a function of layer number in a 3C in 2H SiC superlattice with 1, 6, and 12 cubic layer thickness. Although the potentials change strongly between the Si and the C layers, the potentials change very little from Si to Si (or C to C) layer. By filtering out the rapid atom to atom variation of the potential within a given unit cell, we can focus on the slowly varying potential profile due to interface charge accumulation and dipole resulting in the spontaneous polarization

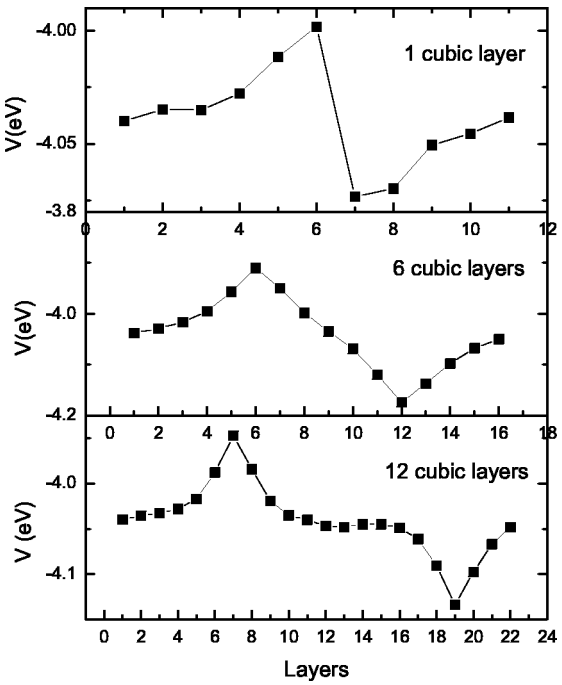

FIG. 3. The profile of the electrostatic potential for HCSL's with 1, 6, and 12 cubic layer inclusions.

slope of the potential and band offset, respectively. To this end one might average the Si and C potentials at the muffin-tin radius or use any other kind of ''local reference level.'' For simplicity, we here simply pick the potential at the Si muffin-tin radius as the ''local reference level.'' For one cubic layer HCSL, the potential changes abruptly at the cubic layer by about 0.08 eV. For six layer 3C HCSL, an almost linear potential profile can be seen in the 3C region. The potential changes by about 0.3 eV between the end points. This is smaller than six times the potential change for one cubic layer inclusion. The potential for 12 layer HCSL shows a completely different profile. Apparently, the potential is not linearly dependent on the distance. In fact, the profile is almost flat in the center part of the 3C region, indicating a strong screening of the potential or spreading out of the interface charges and a reduction of the spontaneous polarization induced potential variation. The total potential change between the two end points is only 0.2 eV, which is smaller than that of the six layer system. We see that the polarization effect becomes smaller with increasing thickness of the 3C inclusion. The length scale over which the screening occurs appears to be between 6 and 12 atomic layers. One may note that even in the six layer case, the ten layer thick 2H part shows a screening of the potential, which is no longer a straight line. These calculations indicate that a significant redistribution of charge and spreading of the interface charge occurs and that the simple macroscopic concept that the interface charge would be a delta-function type sheet of charge of magnitude $\Delta\mathbf{P}\cdot\mathbf{n}$ is not applicable.

The valence band offsets can be calculated by lining up the potential at the Si or Al muffin-tin sphere far away (five to six layers) from the interface with the potential at the Si or Al sphere of the bulk 3C and 2H materials. The VBOs are found to be 0.13 eV for SiC and 0.03 eV for AlN. This is in good comparison with the previous theoretical results.[2,19] The VBO can be separated in a dipole and an intrinsic contribution

$$\Delta E_v(2\mathrm{H}-3\mathrm{C}) = (V_{2\mathrm{H}}-V_{3\mathrm{C}}) + (E_v^{2\mathrm{H}}-V_{2\mathrm{H}}) - (E_v^{3\mathrm{C}}-V_{3\mathrm{C}}),$$
$$= \Delta V_{\mathrm{dipole}} + \Delta E_v^0, \quad (1)$$

where $\Delta V_{\mathrm{dipole}} = V_{2\mathrm{H}} - V_{3\mathrm{C}}$ is the difference in ''local reference level'' in the 2H and 3C part of the supercell, and $E_v^{2\mathrm{H}} - V_{2\mathrm{H}}$ gives the valence band maximum in 2H-SiC relative to that same local reference potential and similarly for 3C. Our calculations show that for sufficiently large cells the dipole contribution is zero. Conceptually, we can attribute part of the intrinsic contribution to the crystal field splitting. The Γ_{15} level at the top of the 3C valence bands splits into a Γ_1 (singlet) and Γ_5 (doublet) if the cubic symmetry is reduced to trigonal or hexagonal symmetry. The energy difference $\Delta_c = E_{\Gamma_5} - E_{\Gamma_1}$ is called the crystal field splitting. For SiC, the crystal field splitting is only 0.13 eV. If the center of gravity of the valence band were aligned, one would expect a contribution to the VBO of only 1/3 of this value, i.e., 0.04 eV. The fact that the actual VBO is 0.12 eV indicates that the center of gravity of the valence band maximum manifold does not stay aligned. Rather the Γ_1 of 2H appears to align with the Γ_{15} of 3C. We can thus further separate the intrinsic band offset in a intrinsic band-offset of the *average* valence band maximum and a crystal field contribution

$$\Delta E_v^0 = \Delta \bar{E}_v^0 + \frac{1}{3}\Delta_c \quad (2)$$

and conclude that for SiC, $\Delta \bar{E}_v^0 = 0.08$ eV Interestingly, the crystal field splitting for AlN is 0.23 eV which is significantly larger than the VBO. Again, the dipole contribution is zero if large enough cells are considered. The intrinsic $\Delta \bar{E}_v^0 = -0.20$ eV in this case is opposite in sign to that in SiC and much larger in magnitude. Interestingly, we note that c/a in 2H SiC is larger than the ideal value $\sqrt{8/3}$ while for AlN, it is smaller but it is not clear whether this is correlated with the present findings or not. Correspondingly, u is larger than the ideal value 3/8 in AlN. While the behavior of the splittings with c/a and u are well understood in terms of so-called deformation potentials,[20] the behavior of the intrinsic $\Delta \bar{E}_v^0$ is not clearly understood in terms of a simple model.

To study the quantum confinement effect, we first line up the potential on the Si or Al sphere of bulk 3C (2H) with the potential on the Si or Al sphere in the middle of the cubic (hexagonal) region in the superlattices. The difference between the conduction band minimum (CBM) of the SL and that of bulk 3C aligned in the above manner is due to the quantum confinement effect. The difference between the CBM of 3C and that of 2H is the well depth. The well depth is found to be 0.704 eV for SiC and 0.725 eV for AlN. Figures 4(a) and 4(b) show the energy levels of the bound states in the well for SiC and AlN, respectively. Surprisingly, these two figures look very similar to the $\mathbf{k}\cdot\mathbf{p}$ calculation results for $Ga_{0.47}In_{0.53}As/Al_{0.48}In_{0.52}As$ (Ref. 21) but on a

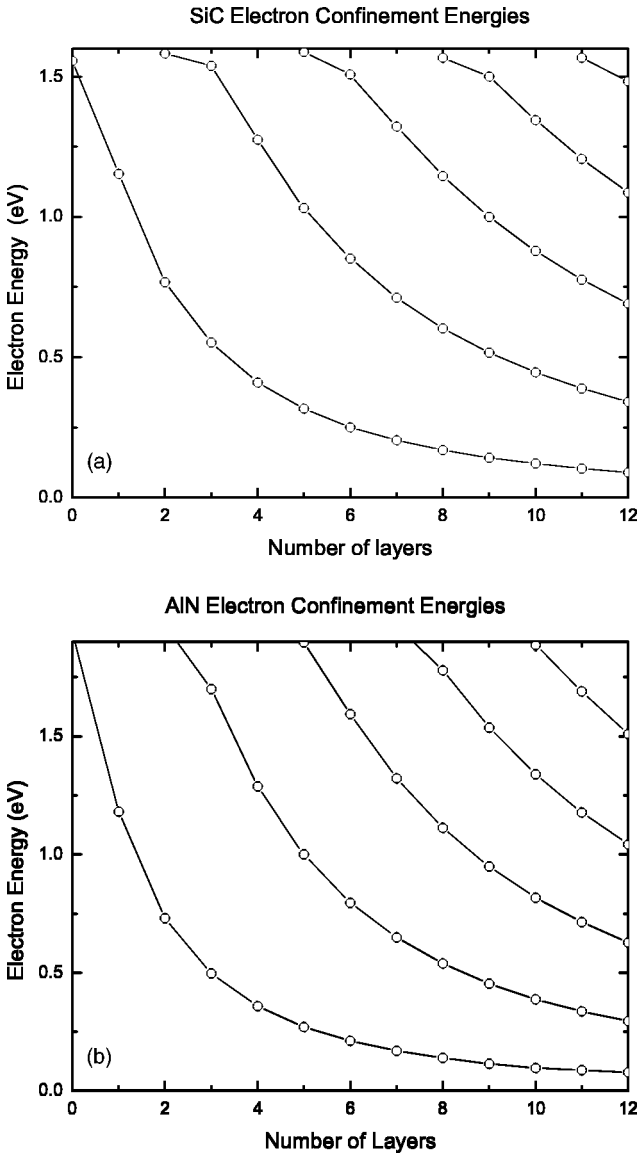

FIG. 4. The energy levels of the bound states in (a) SiC and (b) AlN HCSL's.

much smaller length scale. We note that 12 layers of SiC correspond to about 30 Å . The number of bound states in the well can be explained by a simple quantum well model with finite well depth. If the effective mass is m^*, the well width is a and the well depth is U, the wave vector of the nth state satisfies the following equation:[22]

$$ka = n\pi - 2\sin^{-1}\left[\frac{k\hbar}{\sqrt{2m^*U}}\right].$$

The number of bound states in the well n depends on the parameters $m^*, U,$ and a as

$$\sqrt{2m^*U}a \geqslant (n-1)\pi\hbar$$

and is closely related Heisenberg's uncertainty principle. It can be easily seen from the above criterion that there is always one bound state in the well. Each time the well width increases by another $\pi\hbar/\sqrt{2mU}$, a new bound state will enter the well. For SiC this length is about five layers which is a bit larger than the first principle results. For a $Ga_{0.47}In_{0.53}As/Al_{0.48}In_{0.52}As$ system the effective mass is about 0.045 and the well depth is 0.4 eV. So the critical length is about 45 Å , a value very close to the $\mathbf{k}\cdot\mathbf{p}$ result.

Although a simple quantum well model can estimate the number of bound states in the well, it is not accurate enough for other qualitative properties, for example the spatial decay rate of the quantization energy with well thickness. The simple quantum well always give $E \sim L^{-2}$. However, the energy levels in Fig. 4 appear to be fitted better by an $e^{-\alpha\sqrt{L}}$ behavior for large L. This faster than L^{-2} decay is probably due to the tunneling between the neighboring wells in the superlattice.

Since the confinement quickly decreases with the increasing layer thickness while the VBO is not changed, it is reasonable to expect a gap slightly smaller than bulk 3C for a HCSL with wide 3C and 2H regions. This tendency can already be seen for the band gaps of SiC HCSL in Fig. 2. But this gap compression in HCSL is much smaller than observed in Ref. 1 and is the direct result of the VBO, not of the spontaneous polarization effect.

The quasiparticle corrections will drastically change the fundamental band gap as well as the conduction band structure. However, the band offsets will not be significantly changed because the QP corrections will change the gap for different semiconductors in a similar way. Especially for HCSL's, the QP corrections are quite similar for the different polytypes.[23–26] While keeping the VBM unchanged, the QP corrections to the lowest conduction band levels are parallel and all about 1.2 eV (see Fig. 3 in Ref. 26). Actually, the LDA gaps for various polytypes agree very well with the experimental values after adding a 1 eV QP corrections.[27] Thus, it is unlikely that the QP corrections will change the electronic properties of the superlattice revealed in this paper.

In conclusion, we studied the SiC and AlN 3C/2H heterocrystalline superlattices with a sequentially increasing number of layers in the 3C region. For all the systems we calculated, the fundamental band gap is larger than that of bulk 3C. The polarization of the electrostatic potential was found to be screened and suppressed while the 3C region increases. Although the confinement of quantum well decreases with the increasing well width, the total effect of the polarization and the confinement gives a gap larger than that of 3C for the superlattices thin enough so that the VBO effect does not dominate, i.e., up to at least 12 layers. The energy levels of the bound state in the quantum well resemble a pattern similar to that for the GaAs based quantum wells and superlattices but at an almost 10 times smaller length scale. This indicates that the simple quantum well model and the $\mathbf{k}\cdot\mathbf{p}$ approach should work well for these very thin superlattice systems, providing that the quantum well depth is much higher and the effective mass is significantly larger.

The calculations were performed on the Bewolf AMD cluster at the Ohio Supercomputing Center (OSC) under Project No. PDS0145.

[1] F. Bechstedt and P. Ká̀ckell, Phys. Rev. Lett. **75**, 2180 (1995).
[2] San-huang Ke, Jian Zi, Kai-ming Zhang, and Xi-de Xie, Phys. Rev. B **54**, 8789 (1996).
[3] A. Fissel, U. Kaiser, B. Schröter, and W. Richter, Appl. Phys. Lett. **77**, 2418 (2000).
[4] A. Fissel, U. Kaiser, B. Schröter, W. Richter, and F. Bechstedt, Appl. Surf. Sci. **184**, 37 (2001).
[5] P. O. A. Persson, H. Jacobson, J. M. Molina-Aldareguia, J. P. Bergman, T. Tuomi, W. J. Clegg, E. Janzen, and L. Hultman, Mater. Sci. Forum **389**, 423 (2002).
[6] R. E. Stahlbush, J. B. Fedison, S. D. Arthur, L. B. Rowland, J. W. Kretchmer, and S. Wang, Mater. Sci. Forum **389**, 427 (2002).
[7] T. A. Kuhr, J. Liu, H. J. Chung, M. Skowronski, and F. Szmulowicz, J. Appl. Phys. **92**, 5863 (2002).
[8] H. J. Chung, J. Q. Liu, and M. Skowronski, Appl. Phys. Lett. **81**, 3759 (2002).
[9] L. J. Brillson, S. Tumakha, G. H. Jessen, R. S. Okojie, M. Zhang, and P. Pirouz, Appl. Phys. Lett. **81**, 2785 (2002).
[10] M. S. Miao, S. Limpijumnong, and W. R. L. Lambrecht, Appl. Phys. Lett. **79**, 4360 (2001).
[11] H. Iwata, U. Lindefelt, S. Öberg, and P. R. Briddon, Phys. Rev. B **65**, 033203 (2002).
[12] H. Iwata, U. Lindefelt, S. Öberg, and P. R. Briddon, J. Appl. Phys. **93**, 1577 (2003).
[13] Walter R. L. Lambrecht and M. S. Miao (unpublished).
[14] M. Methfessel, M. van Schilfgaarde, and R. A. Casali, in *Electronic Structure and Physical Properties of Solids, The Uses of the LMTO Method*, edited by Hugues Dreyssé, Springer Lecture Notes, Workshop Mont Saint Odille, France, 1998 (Springer, Berlin, 2000), pp. 114–147.
[15] L. Hedin and B. I. Lundqvist, J. Phys. C **4**, 2064 (1971).
[16] O. Madelung, M. Schulz, and H. Weiss, in *Semiconductors, Physics of Group IV Elements and III-V Compounds*, edited by K. H. Hellwege and O. Madelung, Landolt-Börnstein, New Series, Group III, Vol. 17, Pt. a (Springer-Verlag, Berlin, 1982).
[17] R. G. Humphreys, D. Bimberg, and W. J. Choyke, Solid State Commun. **39**, 163 (1981).
[18] W. R. L. Lambrecht and B. Segall, in *Properties of Group III Nitrides*, edited by J. H. Edgar, EMIS Datareviews Series, No. 11 (the Institution of Electrical Engineers, London, UK, 1994), pp. 135–140.
[19] A. Qteish, V. Heine, and R. J. Needs, Phys. Rev. B **45**, 6534 (1992).
[20] K. Kim, W. R. L. Lambrecht, B. Segall, and M. van Schilfgaarde, Phys. Rev. B **56**, 7363 (1997).
[21] G. Bastard, J. A. Brum, and R. Ferreira, *Solid State Physics* (Academic, San Diego, CA, 1991), Vol. 44, pp. 229–415.
[22] L. D. Landau and E. M. Lifshitz, *Quantum Mechanics* (Pergamon Press, London, 1958).
[23] M. Rohlfing, P. Krüger, and J. Pollmann, Phys. Rev. B **48**, 17791 (1993).
[24] W. H. Backes, P. A. Bobbert, and W. van Haeringen, Phys. Rev. B **51**, 4950 (1994).
[25] Bernd Wenzien, Peter Käckell, Friedhelm Bechstedt, and Giancarlo Cappellini, Phys. Rev. B **52**, 10 897 (1995).
[26] R. T. M. Ummels, P. A. Bobbert, and W. van Haeringen, Phys. Rev. B **58**, 6795 (1998).
[27] W R. L. Lambrecht, S. Limpijumnong, S. N. Rashkeev, and B. Segall, Phys. Status Solidi B **202**, 5 (1997).